Estimating Magma Decompression Rates of the 3600 yr. BP Plinian Eruption of Cerro Machin Volcano, Colombia

MaKayla Etheredge

November 29th, 2021

Dr. Megan Newcombe, Silvia Castilla Montagut

GEOL394

Abstract

Bubbles in pumice provide a frozen record of the physical state of magma in volcanic conduits during Plinian eruptions. Bubble formation increases magma buoyancy, which is the driving force behind explosive eruptions. It is thought that the number and size of bubbles in pumice may relate to the decompression rate of magma during syneruptive ascent: Rapid magma decompression leads to a relatively high degree of volatile supersaturation in the melt, which encourages the nucleation of many small bubbles and produces pumice with a high bubble number density (i.e., a relatively large number of bubbles per unit volume of pumice); conversely, slow magma decompression allows bubbles to nucleate and grow at a lower degree of volatile supersaturation, thereby producing pumice with low bubble number density. For this reason, bubble number density (BND) in pumice has been developed as a useful tool for estimating magma decompression rates during volcanic eruptions. The MATLAB application FOAMS (Shea et al., 2010) and decompression rate meter (Toramaru, 2006) were used to calculate BND and magma decompression rates during the 3600 yr. BP Plinian eruption of Cerro Machin Volcano. Pumice clasts from the base, middle, and top of this deposit were characterized in order to test whether the BND of the pumices changed systematically over the course of the eruption. BNDs of a pumice clast sampled from the base of the deposit (i.e., erupted during the opening phase of the eruption) record a magma decompression rate of 6.5 $\pm$ 0.52 MPa/s, while pumices from the middle and top layers record 2.8$\pm$ 0.28 MPa/s and 2.5$\pm$ 0.17 MPa/s, respectively. These results indicate that the magma decompression rate decreased over time, demonstrating the waning of the volcanic eruption.

Table of Contents

1) Introduction

1.1 Plinian Eruptions and Decompression Rates

A qualitative understanding of the dynamics of volcanic eruption is poorly constrained. This is due to volcanologists not being able to directly measure the interior of the conduit during eruptions. Processes that happen during volcanic eruptions such as magma decompression are important in understanding how a volcano might erupt. Magma decompression rates can be used to tell whether a volcanic eruption will erupt explosively or effusively (Cassidy et al., 2018). Magmas that decompress at rates over ~0.1 MPa/s typically erupt explosively, while magmas with decompression rates under ~0.1 MPa/s typically erupt effusively (Figure 1). In basaltic to intermediate systems, scientists have found that magma decompression rates correlate with mass eruption rates; this result is suggestive of a direct link between decompression rate and eruptive style (Barth et al., 2019). Plinian volcanic eruptions are destructive events that have many associated hazards such as pyroclastic flows and lahars. Fortunately, these catastrophic eruptions are rare; however, their rarity means that very few Plinian eruptions have been observed using modern scientific instrumentation. Considering the paucity of real-time observations of these events, we must instead turn to the rock record in order to understand the mechanisms and impacts of Plinian eruptions. With this study, I have examined the rock record to quantify magma decompression rates at Cerro Machin during the 3600 yr. BP Plinian eruption. This has allowed for a better understanding of Cerro Machin eruption patterns and potential hazards that future eruptions may pose.

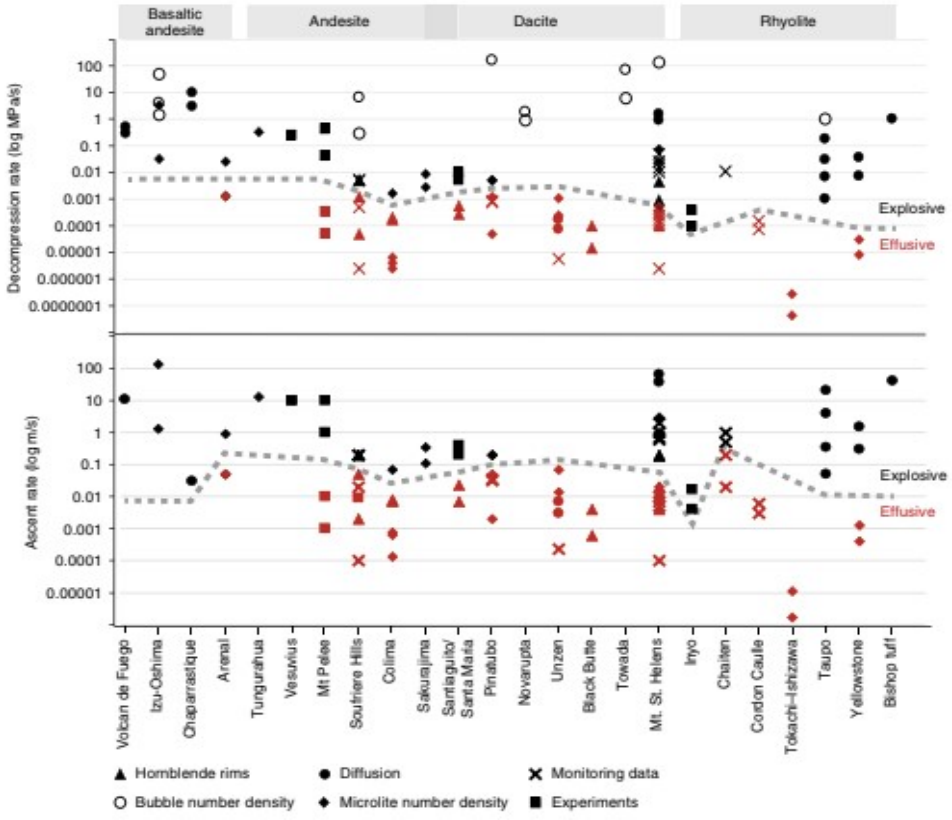

Figure 1: Plot of Volcanic Eruptions vs Decompression and Ascent Rates (Cassidy et al., 2018). The graph showcases the differences in decompression rates of effusive and explosive eruptions. The graph displays how magmas with decompression rates over ~0.1 MPa/s typically erupt explosively, while magmas with decompression rates under ~0.1 MPa/s typically erupt effusively. Decompression rates were found using different methods such as bubble number density, diffusion, and microlite number density.

2.) Geological Background

2.1 Geological Setting

Cerro Machin Volcano is a stratovolcano located in Colombia, South America. Cerro Machin is considered to be one of Colombia's most dangerous volcanos because of its demonstrated ability to bring about major explosive eruptions and vicinity to densely populated cities (Laeger et al., 2013). Within the last 5000 years, Cerro Machin has produced at least six large dacitic eruptions which included four Plinian, one Sub-Plinian, and one Vulcanian eruption. These eruptions occurred ~5000, ~4600, ~3600, ~2600, ~1200, and ~900 years ago. These ages were determined using C^{14} radiometric dating of associated charcoal layers (Londono, 2016). These eruptions produced hazardous pyroclastic flows, pyroclastic falls, and lahars. Cortes (2001) reports that out of the six eruptions, five generated lahars. One of the lahars described by Cortes (2001) as the Chircoal Flow Deposit, reached over 100 km from the vent. Products of all the eruptions reached areas currently inhabited by occupants of the capital cities of Ibagué and Armenia, and the towns of Calarcá, Cajamarca, and Anaime. If a volcanic eruption were to happen today, it would affect nearly one million people.

Figure 2.1: Picture of Cerro Machin Volcano, Colombia (Cortes, 2001).

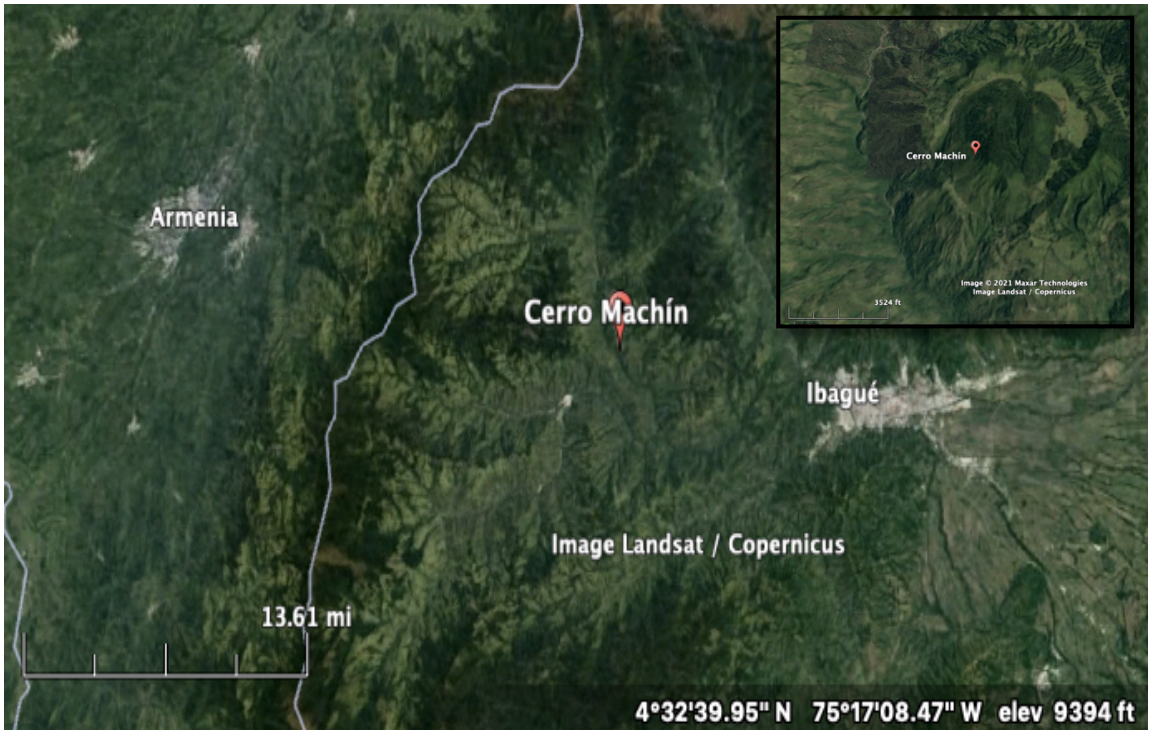

Figure 2.1.2: Google map image of surrounding area near Cerro Machin Volcano, Colombia. Nearby cities such as Ibague and Armenia are shown.

While there have been studies examining Cerro Machin Volcano, there has been a lack of research surrounding the intra-conduit processes of the volcano during eruptions. More specifically, magma decompression rates have not yet been constrained for Cerro Machin eruptions. The 3600 yr. BP eruption of Cerro Machin is thought to have been a Plinian eruption based on characterization of its pyroclastic deposits (Galeano, 2005). Quantifying magma decompression rates throughout one of Cerro Machin's major volcanic eruptions would hold great significance in understanding the destructive patterns of the volcano.

2.2 Bubble Number Density and Decompression Rates

Volcanologists currently use many different methodologies to quantify magma decompression rates. The use of bubble textures in pumice has shown to be effective through many studies (Toramaru 2006; Shea et al., 2010; Shea 2017). More specifically, BND in pumice has been successfully used to constrain magma decompression rates (Myers et al., 2021). During a volcanic eruption, nucleation of bubbles occurs due to the decrease in pressure as magma rises to the surface. Dissolved volatiles become supersaturated and cause bubbles to nucleate. Because nucleation rate increases with supersaturation, BND from individual pumice clasts can be used to estimate magma decompression rates. Rapid magma decompression leads to volatile supersaturation in the melt, encouraging the nucleation of many tiny bubbles, leading to high bubble number density. Conversely, slow magma decompression allows bubbles to nucleate and grow at lower degrees of volatile supersaturation, producing magma with low bubble number density. (Figure 2.2)

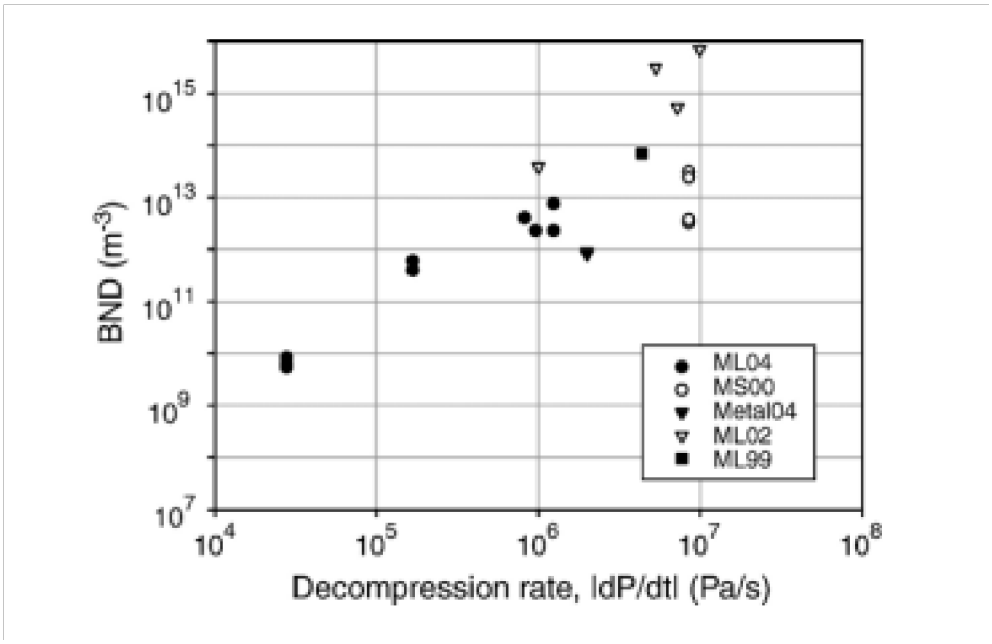

Figure 2.2: Toramaru (2006) graph plots Magma Decompression Rate vs Bubble Number Density (BND). The graph demonstrates that BND is a function of magma decompression rate. BNDs were taken from previous studies. Toramaru (2006) calculated magma decompression rates from these eruptions using his BND decompression rate meter equation.

To help quantify decompression rates from bubble number density, Toramaru (2006), developed a decompression rate-meter guide that links the number density of bubbles per unit volume melt (N) in pyroclasts to rates of magma decompression (dP/dt) during ascent. The model was calibrated using decompression experiments and has been used to calculate decompression rates of many eruptions. By calculating BND from three different phases of a Plinian eruption of Cerro Machin using the MATLAB application FOAMS (Shea et al., 2010), the decompression rate-meter equation (Toramaru, 2006) can be used to estimate magma decompression rates throughout the eruption.

2.3 Bubble Number Density Uncertainties

The use of Bubble Number Density in pumice clasts to estimate decompression rates is associated with several sources of uncertainty. If there is variability of BND within the pumice, there might be sources of error. One example being bubble number density relies on the idea that the pumice rapidly quenches after exiting the conduit. However, the centers of the larger pumice clasts may quench relatively slowly due to the time taken for heat to conduct across the diameter of the clast. This slow quench may allow post-eruptive bubble growth, which may introduce error in our results, because the pumice texture may not reflect bubble growth in the conduit. By separately calculating BND from the inside and outside of Cerro Machin's pumice clasts, I can examine my results to see if there is variability of BND in the pumice clasts.

3.) Objective:

The goal of this study was to estimate magma decompression rates of Cerro Machin's 3600 yr. BP eruption. This study will analyze approximate bubble number density (BND) from Cerro Machin pumice and compute magma decompression rates using the decompression rate meter (Toramaru, 2006) for the beginning, middle, and end of the 3600 yr. BP eruption. I will test two hypotheses: My first hypothesis is that the center of the pumice clasts will have a different BND than the edge of the pumice due to perhaps post-eruptive bubble growth. My second hypothesis is that the magma decompression rate will decrease over the course of the eruption. This may be due to the overpressure being released and the eruption waning over time. This study will help to increase research of Cerro Machin volcano and its associated hazards; and will provide insight into conduit processes during explosive dacitic eruptions.

4.) Methods

4.1 Sampling Cerro Machin Pumice

Silvia Castilla Montagut collected pumice in October 2020 from Cerro Machin's 3600 yr. BP fall deposit. The fall deposit is located 9 kilometers from the vent. Silvia Castilla Montagut followed the interpretation of Cerro Machin 3600 yr. BP eruption discussed in Galeano (2005). Galeano (2005) did an intensive study of all of Cerro Machin fall deposits and pyroclastic flows. Galeano (2005) found Cerro Machin's 3600 yr. BP eruption was one continuous eruption that erupted for fifty-four hours total based on the lithology, location, and grading bedding. He used the idea of graded bedding in the fall deposits to demonstrate that Cerro Machin was one continuous eruption. He says there was the initial explosion and the finer material ejected was carried laterally away from the conduit due to the wind. Most of the denser pumice clasts deposited closer to the vent due to weight. As the eruption continued, its energy waned; this transition is reflected in the bedding which grades from large clasts to finer clasts (Fig. 4.1).

Figure 4.1: Photo of Cerro Machin's 3600 yr. BP fall deposit. The fall deposit is outlined in red. The fall deposit showcases fining upwards or graded bedding. Scale is in centimeters. Photo from S. Castilla Montagut.

Silvia Castilla Montagut used this interpretation and sampled pumice clasts from the three separate layers of the 3600 yr. BP volcanic fall deposit (Figure 4.1.2). She split the fall deposit into three equal sections which are the bottom layer, middle layer, and top layer. These three layers represent the beginning, middle, and end of the eruption. One pumice clast from each layer with a total of three pumice clasts were chosen for this study. The pumice clasts were analyzed to ensure they were not altered from the original state (i.e. disregarding abnormally oblong pumice clasts).

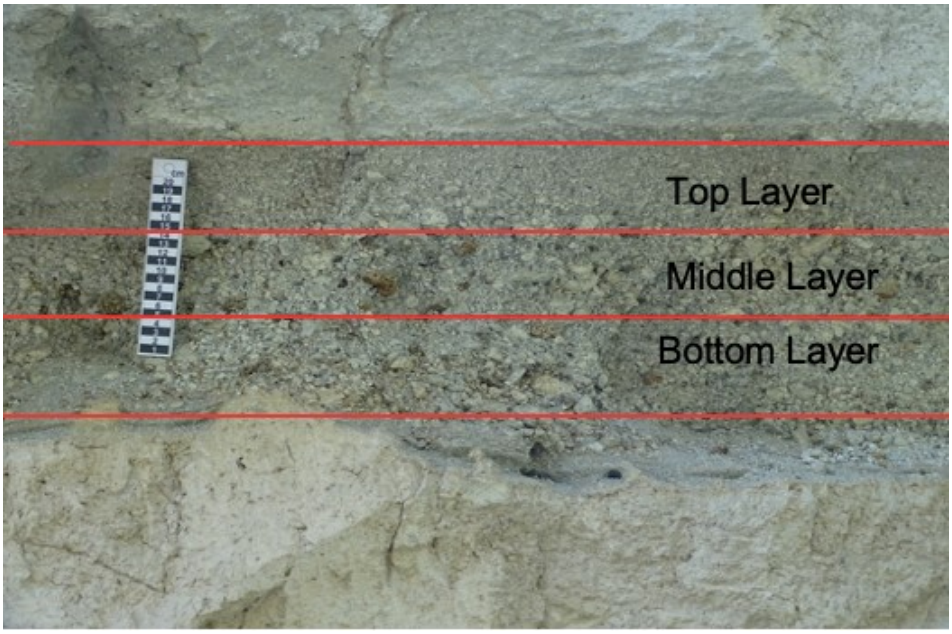

Figure 4.1.2: This image shows Cerro Machin's 3600 yr. BP fall deposit split up into 3 equal layers (red lines) by Silvia Castilla Montagut. The scale is in centimeters.

4.2 Imaging

For this study, I took Backscattered Electron (BSE) images of three clasts of pumice using a JEOL JXA-8900R Electron Probe Microanalyzer with assistance from Dr. Phillip Piccoli. Bubble sizes in the pumices span several orders of magnitude (from microns to centimeters in diameter), so we applied the nested imaging technique proposed by Shea et al. (2010) to ensure that we counted bubbles across this entire size range. Images taken at high magnification (>450x) found the smallest bubble to be ~1 micron in diameter, from which it was determined that the highest magnification needed to capture the smallest bubble was 450x. Applying the nesting method from Shea et al. (2010), there was a collection of images at magnifications of 50x, 250x, and 450x. In order to test whether the centers of the pumices were different from the edge, I compared 7 images of the edges and 7 images of the centers of each pumice clast from each layer (Figure 4.2).

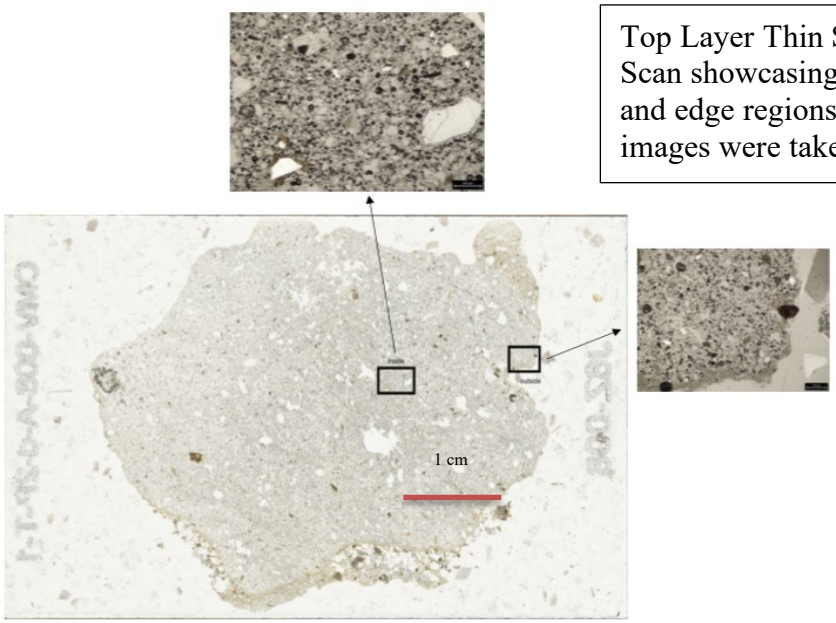

Top Layer Thin Section Scan showcasing the center and edge regions of where images were taken.

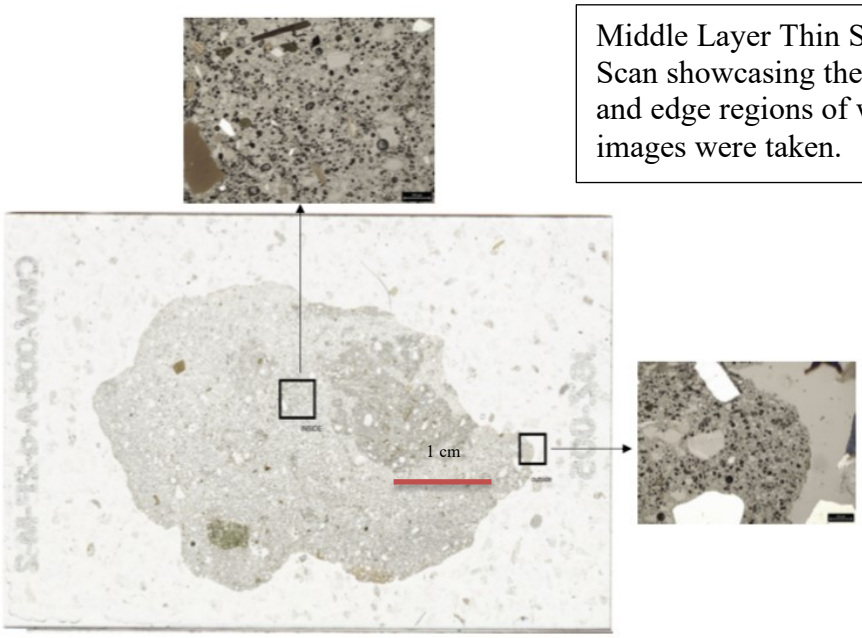

Middle Layer Thin Section Scan showcasing the center and edge regions of where images were taken.

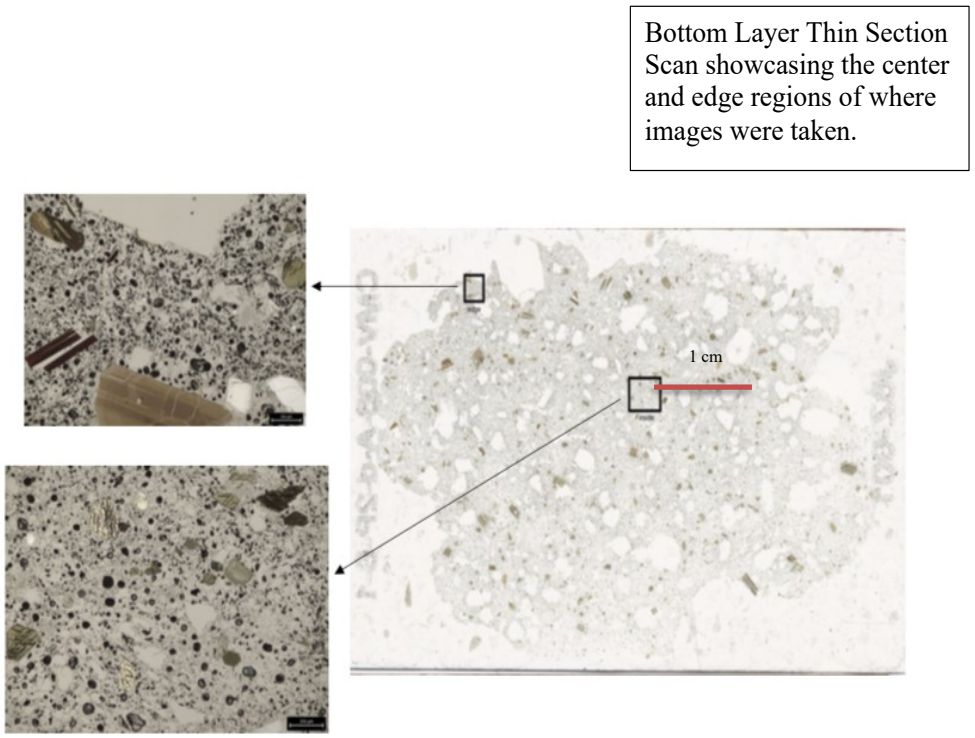

Figure 4.2: Thin Section Scans of the pumice clast from each of the three layers. The black boxes in each image show where the photomicrographs for the center and edge of the pumice were taken.

Shea et al. (2010) used Adobe Photoshop to edit his images to allow FOAMS to accurately record the bubble size. FOAMS requires grayscale; therefore, bubbles must be black and everything else in the matrix should be gray or white. This was completed in this study by first applying a black and white filter to the images using the software package Fiji. Adobe Photoshop and Illustrator were then used to fill in the bubbles to black, and everything else (minerals, glass) was filled in to be white. All the edited 450x images that captured the smallest bubbles are shown in Figure 4.2.2. There is a clear difference of BND from the beginning and end of the eruption, with the beginning visibly having a higher BND.

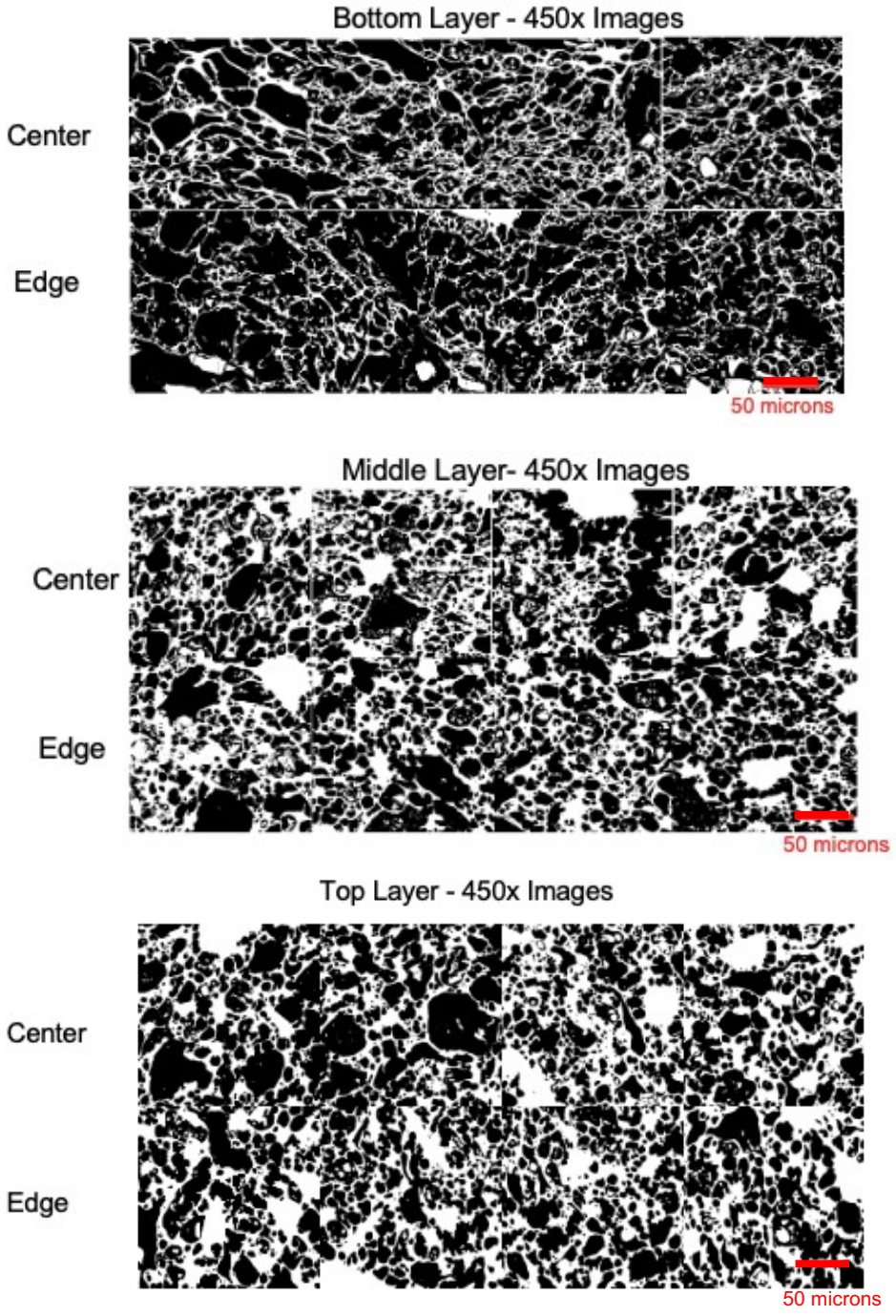

Figure 4.2.2: Edited 450x Backscattered Electron Images. The total number of 450x images was 8 for each pumice clast analyzed.

4.3 FOAMS Calculation of BND

FOAMS or Fast Object Acquisition Maintenance System is a MATLAB application developed by Shea et al. (2010) that quantifies different characteristics of bubbles in pumice. When provided with a set of images of a pumice clast, FOAMS performs a vesicle count and calculates a vesicle volume in order to produce a bubble number density. FOAMS also calculates the number density of objects of a given size per unit volume, NAi. NAi is the number density per unit area and is calculated using an expression that estimates the probability of intersecting spheres of given sizes through their maximum cross-sectional area. Shea et al. (2010) based these calculations on the work of Underwood (1970) who obtained NVi and NAi by introducing a parameter called the mean projected height (HP0, mm), which represents the mean distance between parallel planes tangential to the object boundary. For spherical objects, this equates to the characteristic diameter of each size class (L, mm). The diameter is then used to correct NA values for intersection probabilities based on the stereological assumption NV = NA (Underwood, 1970), and then corrected for the cut-effect to calculate final number densities (Nvi, mm^{-3}) and volumes of equivalent spheres (Vi, mm^3).

There were a series of experiments done to test both hypotheses. To test the first hypothesis, FOAMS was used to calculate BND for the center and edge of each pumice clast. In order to assess the uncertainty on the BND values, there was a series of BND calculations in which the 450x images were removed one at a time (with replacement of the image after each calculation). Calculations of the standard deviation of the BND values obtained from these different image combinations, which I report as the uncertainty on the BND obtained from the complete set of images. The 450x images accounted for the smallest bubbles which according to Shea et al. (2010) have a strong impact on FOAMS calculation of BND. Therefore, getting an accurate read of these small bubbles is important.

For my second experiment, I inputted the images from both the center and edge of the pumice clasts into FOAMS to get a BND for each layer. To account for uncertainties again, I substituted the 450x images out in order to get a series of BND calculation results from FOAMS and I calculated the standard deviation of the BND values as an assessment of the uncertainty. The mean average of all BNDs from each layer were taken to calculate magma decompression rates for each layer.

4.4 Calculation of Magma Decompression Rates

After acquiring BND values using FOAMS, I was able to calculate decompression rates using a parameterization developed by Toramaru (2006). This decompression rate-meter (Equation 4.4) links the number density of bubbles per unit volume melt (N) in pyroclasts to rates of magma decompression (dP/dt) during ascent. In order to develop this, Toramaru (2006) did a series of experiments where he put natural magma into a furnace, heated it up to high temperatures and pressures, decompressed it at a known rate, then quenched it. He then measured BND. The model was calibrated using these experiments and has been used to calculate decompression rates of many eruptions with a range of magma compositions.

$$\frac{|dP|}{|dt|} = a \cdot D \cdot \sigma \cdot {P_w}^{-1/3} \cdot T^{-1/2} \cdot N^{2/3}$$

Equation 4.4: The *N* in this equation represents Bubble Number Density in mm^3. The *T* represents temperature of the melt in Kelvin, *P* represents pressure of water in the melt in Pa, and *D* is the diffusivity of H_2O in the melt in m^2s^{-1}. The interfacial tension is represented by o^2 in Nm^{-1} and the constant *a* is equal to 3.5×10^{14}.

a	H20 weight %	Diffusivity (m^2s^{-1})	Interfacial Tension-Heterogenous Magma (Nm^{-1})	Pressure (Pa)	Temperature (K)
3.5×10^{14}	6.1	1.4×10^{11}	0.025	3.6×10^8	1243

Figure 4.4: This table shows the conditions used to calculate magma decompression rates. Laeger et. al (2013) tested the conditions of crystallization of amphiboles in Cerro Machin's 900 yr. BP eruption and found pressure of water during the eruption to be 360 MPa or 3.6×10^8 Pa and temperature to be 970 ºC which is 1243 Kelvin. I can use these numbers to infer constraints for the 3600 yr. BP eruption. The diffusivity of H_2O (D) as a function of temperature, pressure and water concentration can be calculated using the parameterization of Zhang et. al (2007). Assuming a melt H_2O content of 6.1 $\pm$ 0.7 weight percent (Laeger et al., 2013) the diffusivity of H_2O was found to be 1.4×10^{-11} m^2s^{-1}. The interfacial tension variable o^2 takes different values depending on whether vesicle nucleation was heterogenous or homogenous. I estimated decompression rates assuming heterogenous nucleation, where the interfacial tension is 0.25 N m^{-1} (Shea, 2017). The constant *a* is equal to 3.5×10^{14}.

5.) Discussion of Results

5.1 Comparing Center Region BND and Edge BND

The first experiment tested the hypothesis that pumice clasts from Cerro Machin 3600 yr. B.P eruption could record different BND in their centers and at their edges due to perhaps post eruptive bubble growth. Figure 5.1 shows the numbers recorded by FOAMS. FOAMS calculates the same BND of 16.0 m^{-3} for both the center and edge of the pumice sampled from the bottom layer. There is a slight difference in BND for the middle layer with BND from the center being 15.4 m^{-3} and the edge being 15.5 m^{-3}, however, this difference is within the uncertainties of our BND estimates. The top layer also recorded a slightly different BND for both regions with the center being 15.6 m^{-3} and the edge being 15.2 m^{-3}, however, this difference is not within two standard deviations. This layer is statistically significant, however there is a difference in BND with the center being higher and not the edge. I conclude for this experiment that this pumice clast has variability of BND. However, more experiments from each layer are needed to conclude BND variability for each layer.

Layer	Region	Bubble Number Density (BND) ($log10(m^{-3})$)	BND Uncertainty ($log10(m^{-3})$)
Top	Center	15.6	0.02
	Edge	15.2	0.03
Middle	Center	15.4	0.03
	Edge	15.5	0.06
Bottom	Center	16	0.05
	Edge	16	0.08

Figure 5.1: Table showing recorded BND and BND uncertainty from each layer and region of the pumice clast. Standard deviations and uncertainties are of a 1-sigma.

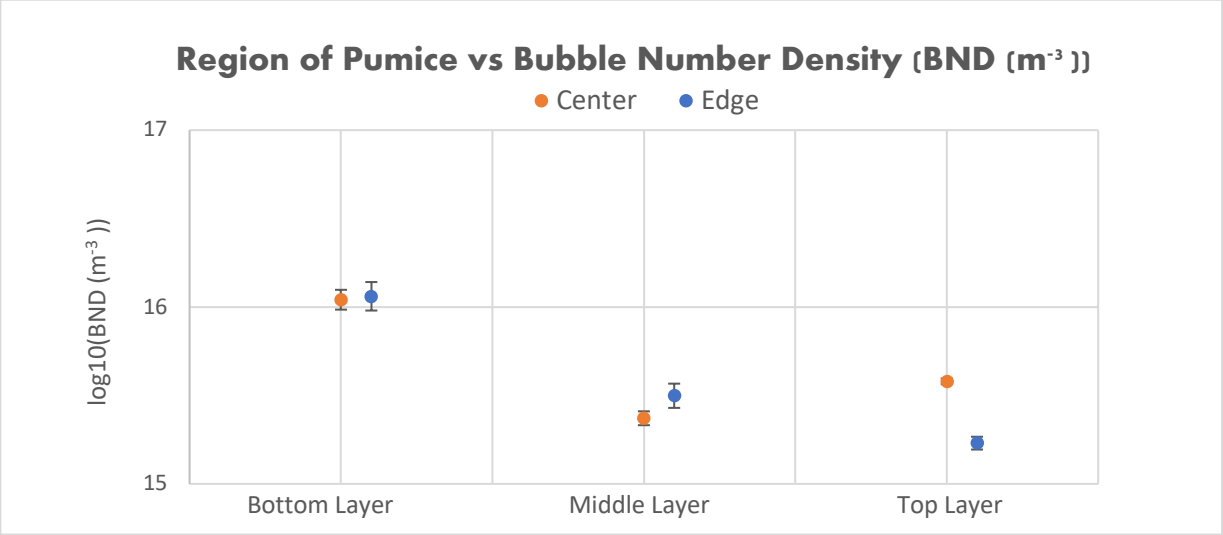

Figure 5.1.2: Graph showing recorded BND vs Region of Pumice from each Layer. Center regions are in blue and edge regions are in orange. BND Uncertainty is shown through error bars.

5.2 Comparing Magma Decompression Rates throughout the Eruption

The second experiment was designed to test the hypothesis that the magma decompression rate decreased over the course of Cerro Machin's 3600 yr. B.P eruption, perhaps in response to the release of overpressure and the eruption waning over time. Pumice from the bottom layer (representing the beginning of the eruption) records a magma decompression rate of

6.5 MPa/s. Pumice from the top layer (representing the end of the eruption), records a magma decompression rate of 2.5 Mpa/s. The result supports my hypothesis that the magma decompression rate decreased significantly over the course of the eruption. For this study, I have defined statistical significance as outside of two standard deviations or uncertainties. My results suggest that the eruption waned over time.

Layer	Magma Decompression Rate (Mpa/s)	Magma Decompression Rate Uncertainty (Mpa/s)
Top Layer	**2.5**	**0.17**
Middle Layer	**2.8**	**0.28**
Bottom Layer	**6.5**	**0.52**

Figure 5.2: Table showing recorded Layer and its corresponding Magma Decompression Rates and Magma Decompression Rate Uncertainty. Standard deviations and uncertainties are of a 1-sigma.

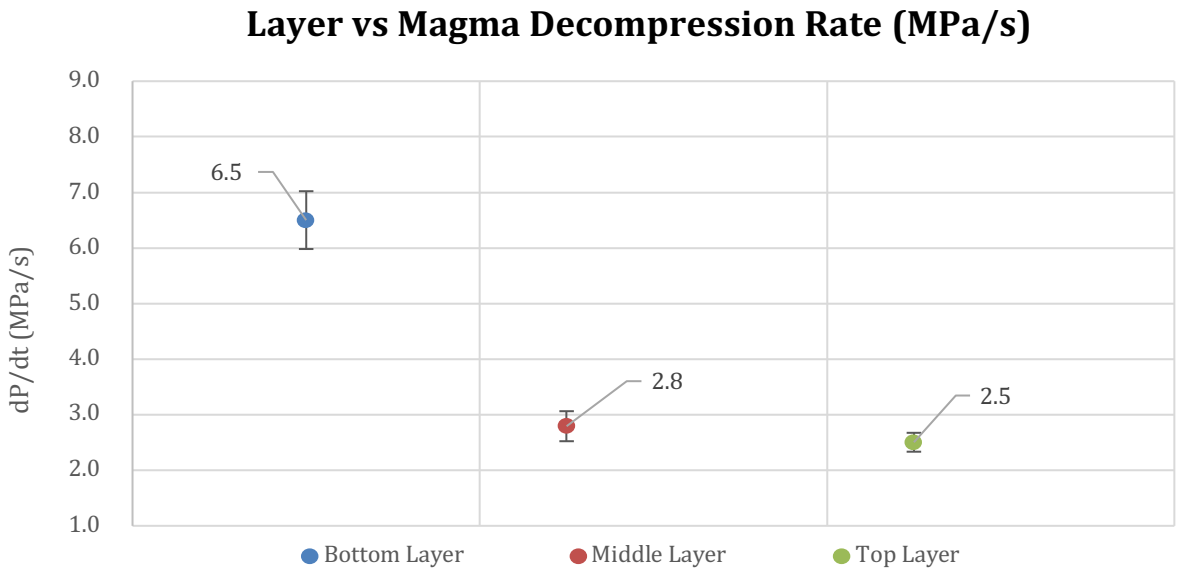

Figure 5.2.2: Graph showing Layer vs corresponding Magma Decompression Rates. Magma Decompression Rate Uncertainty is shown through error bars.

5.3 Comparing Cerro Machin's Magma Decompression Rates to other Eruptions

My results indicate that magma erupted during the opening phase of Cerro Machin's 3600 yr. BP eruption decompressed at a rate of 6.5 MPa/s. This magma decompression rate is over the ~0.1 MPa/s 'threshold' between effusive and explosive behavior defined by Cassidy et al. (2018) (Figure 5.3) and is in good agreement with magma decompression rates obtained for other Plinian eruptions such as the eruption of Mount Vesuvius in 512 A.D: Pumice clasts from Mount Vesuvius' eruption record a magma decompression rate of 4.7 MPa/s (Shea, 2017).

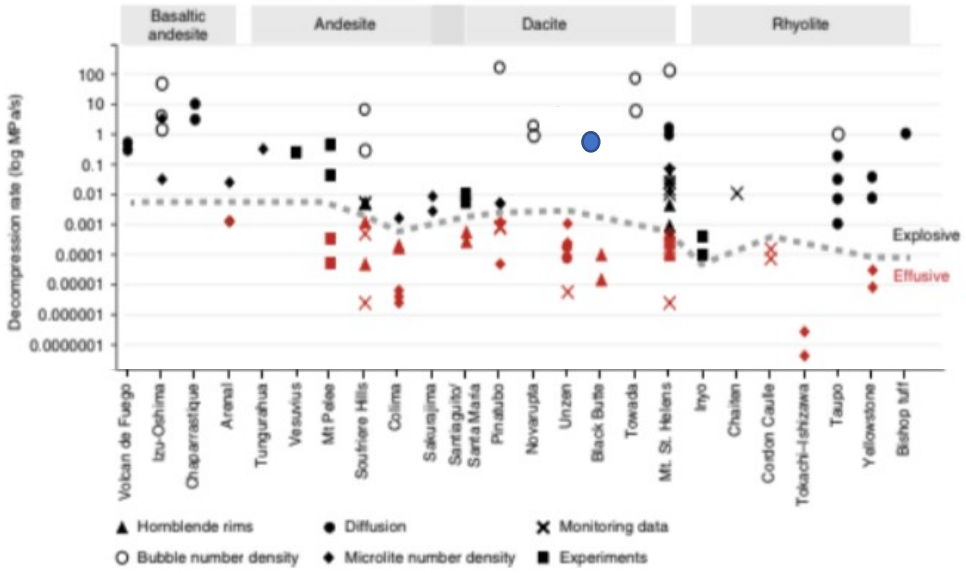

Figure 5.3: Edited Cassidy et. al (2018) Figure. Cerro Machin's 3600 yr. BP beginning magma decompression rate of 6.5 MPa/s is shown by the blue circle. Cerro Machin's magma decompression rate is comparable to other dacitic explosive eruptions.

6) Broader Impacts

This study aimed to increase research surrounding Cerro Machin eruptive processes and associated hazards. The beginning magma decompression rate of Cerro Machin's 3600 yr. BP eruption measured 6.5 MPa/s. Through personal communication with Silvia Castilla Montagut, the magma storage was at ~300 MPa in the conduit based on amphibole barometry. This interpretation has led to the conclusion that if a similar eruption were to happen today at Cerro Machin, it would take a minimum time of 46 seconds for the magma to travel from its source to the surface. This is likely a minimum time estimate because the bubbles record the decompression rate at the top of the conduit, and the magma likely accelerates as it rises to the surface. However, nonetheless, this time suggest that the surrounding cities and towns of Cerro Machin scaling around 1 million people may have limited time to prepare if a volcanic eruption were to happen today. Quantifying more volcanic processes surrounding Cerro Machin would be of importance.

7.) Suggestions for Future work

While the chosen pumice from this study has yielded results, there are other studies (Myers et. al., 2021) that suggest having a range of pumice clasts from each layer might be useful in accurately estimating BND and magma decompression rates. By analyzing a range of pumice clasts from each layer, there might be a chance to get a more robust representation of the average BND throughout each layer. Further work to measure BND for a range of pumice clasts throughout each layer would be valuable.

8.) Conclusion

Bubble number densities in three pumice clasts were measured from a fall deposit of the 3600 yr. BP eruption of Cerro Machin. BNDs at the centers versus the edges of each pumice from the top and middle layer are not significantly different, thereby indicating that the pumices were not significantly affected by post eruptive bubble growth. BNDs at the center versus the edge of the pumice from the top layer are significantly different suggesting variability of BND of the pumice. BNDs of pumices from the base, middle, and top of the 3600 yr. BP deposit indicate magma decompression rates of 6.5 $\pm$ 0.52 MPa/s, 2.8$\pm$ 0.28 MPa/s and 2.5$\pm$ 0.17 MPa/s, respectively. The decrease in magma decompression rate recorded by the BNDs of the pumice clasts indicate that the eruption waned over time, perhaps due to the release of overpressure. Magma decompression rates from Cerro Machin's 3600 yr. B.P. eruption are similar to decompression rates found for other Plinian eruptions. More calculations of bubble number density and magma decompression rates from additional Cerro Machin pumice clasts within each layer will allow a more robust estimate of my uncertainties. With lessening uncertainties, there will be a more accurate representation of Cerro Machin volcanic eruptions and the associated hazards they may pose.

9.) References

Barth A., Newcombe M., Planka T., Gonnermannb H., Hajimirzab S., Sotoc G., Saballosd A., Hauri E., 2019. Magma decompression rate correlates with explosivity at basaltic volcanoes — Constraints from water diffusion in olivine. Journal of Volcanology and Geothermal Research, 387.

Cassidy Mike., Manga M., Cashman K., Bachmann O., 2018. Controls on explosive-effusive volcanic eruption styles. Nature Communications. (9-17).

Cortés, G.P., 2001. Estudio geológico de los depósitos de lahar asociados a la actividad eruptiva del Volcán Cerro Machín. Internal Report. INGEOMINAS, Manizales, Colombia, (96-110).

Galeano H., 2005. Erupciones Pllnianas del Holoceno en el Volcan, Cerro Machin, Colombia, Estratigrafia, Petrografia y Dinamica eruptiva. Universidad Nacional Autonoma de Mexico. (1-129)

Laeger K., Halama R., Hansteen T., Savov d I., Murcia H., Cortés G.,Garbe-Schönberg D., 2013. Crystallization conditions and petrogenesis of the lava dome from the ~900 years BP eruption of Cerro Machín Volcano, Colombia. Journal of South American Earth Sciences. Res. 48, (193-208)

Londono J. Makario., 2016. Evidence of Recent Deep Magmatic Activity at Cerro Bravo-Cerro Machín Volcanic Complex, Central Colombia. Implications for Future Volcanic Activity at Nevado Del Ruiz, Cerro Machín and Other Volcanoes. Journal of Volcanology and Geothermal Research.(156-168).

Myers M., Druitt T., Schiavi1 F., Gurioli1 L., Flaherty T., 2021. Evolution of magma decompression and discharge during a Plinian event (Late Bronze-Age eruption, Santorini) from multiple eruption-intensity proxies. Journal of the International Association of Volcanology and Chemistry of Earth's Interior. 83, (18).

Shea, T., Houghton, B.F., Gurioli, L., Cashman, K.V., Hammer, J.E., Hobden, B.V., 2010. Textural analyses of vesicles in volcanic rocks: an integrated methodology. Journal of Volcanology and Geothermal Research. 190, (271–289).

Shea, T., 2017. Bubble nucleation in magmas: A dominantly heterogeneous process?. Journal of Volcanology and Geothermal Research. 343, (155–170).

Toramaru, A., 2006. BND (bubble number density) decompression rate meter for explosive volcanic eruptions. Journal of Volcanology and Geothermal Research. 154, (303–316).

Underwood, E.E., 1970. Quantitative stereology. Addison-Wesley, (264-274)

Zhang Y., Xu Z., Zhu M.,Wang H.,2007. Silicate melt properties and volcanic eruptions.

9) Appendix

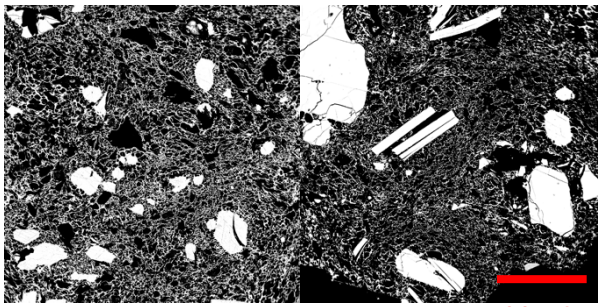

50x Images

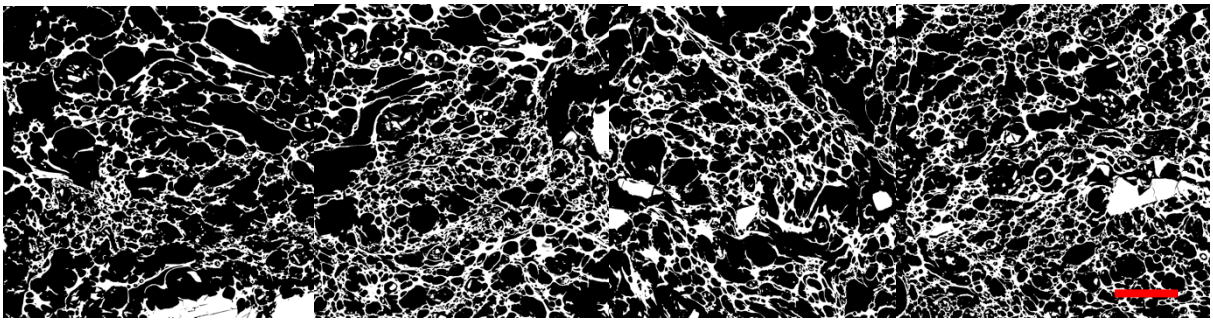

250x Images

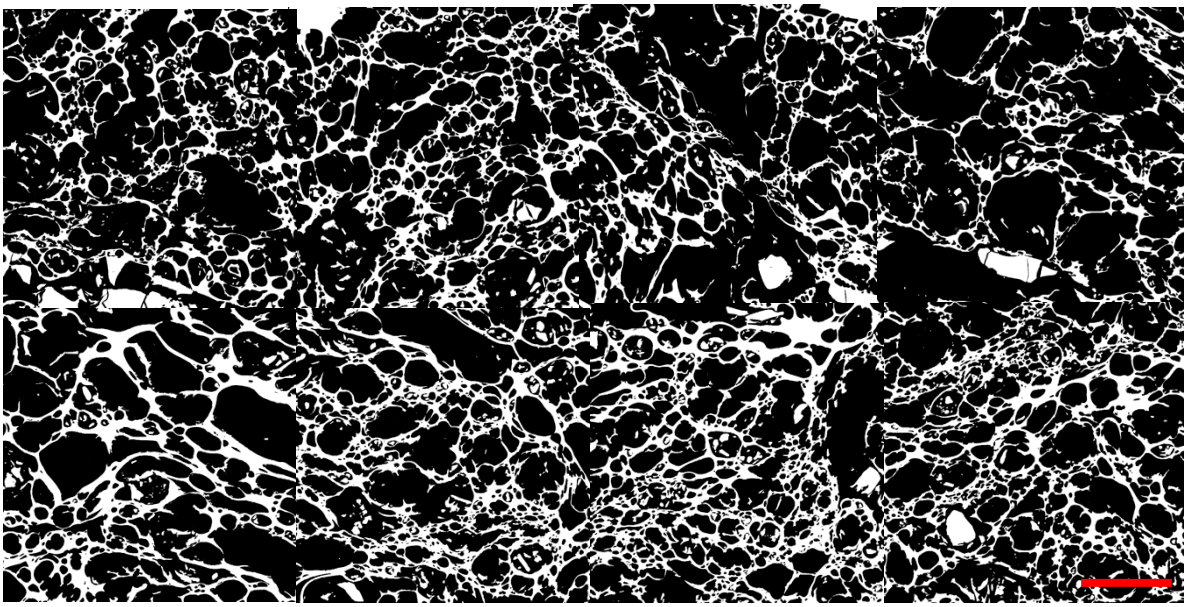

450x Images

Supplementary Figure 1: Edited Backscattered Electron (BSE) images for the bottom layer of the eruption.

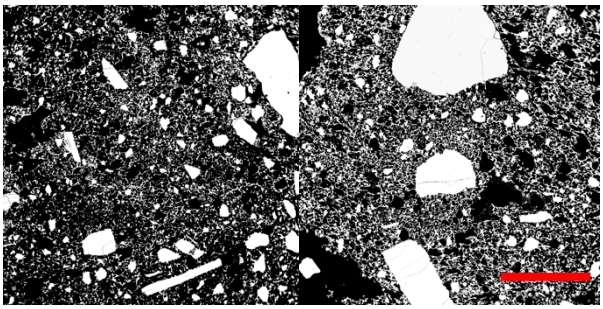

50x Images

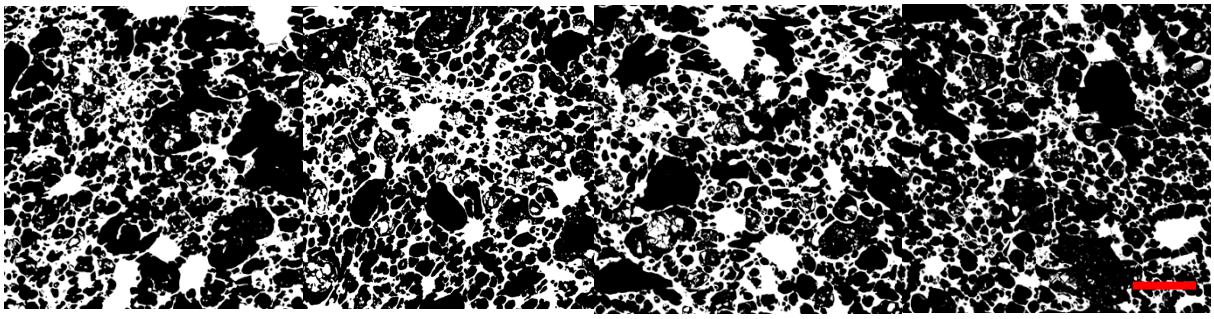

250x Images

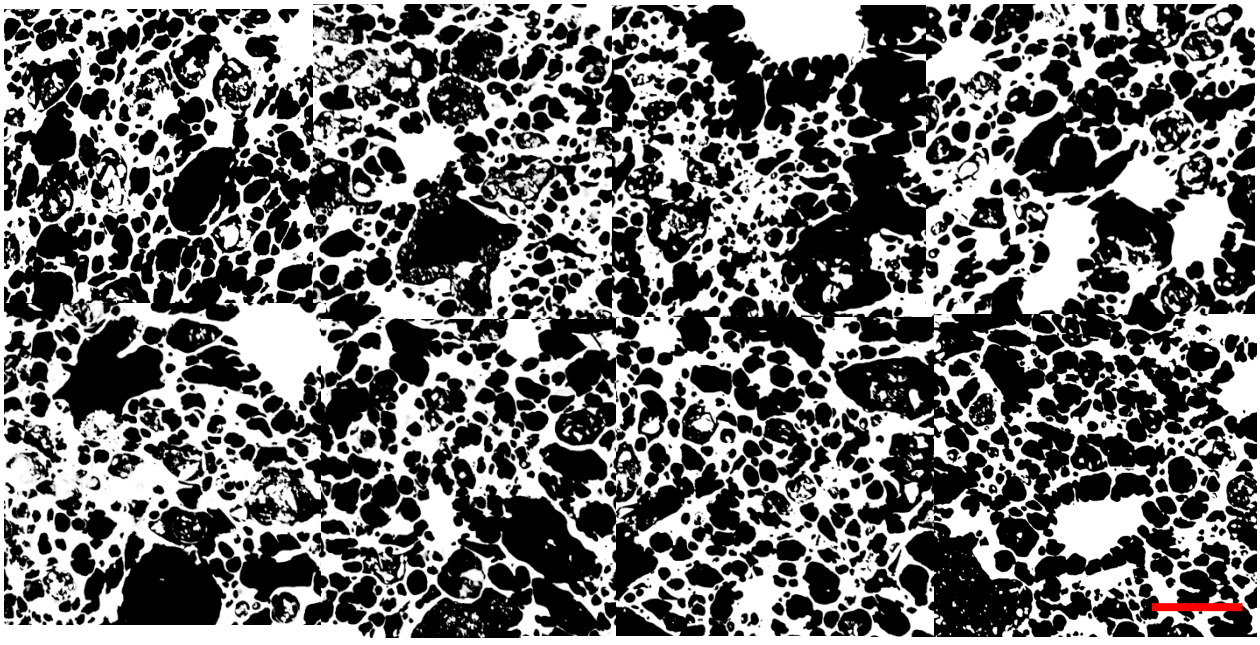

450x Images

Supplementary Figure 2: Edited BSE images for the middle layer of the eruption.

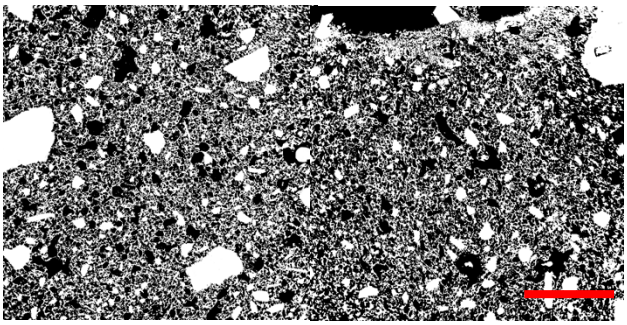

50x Images

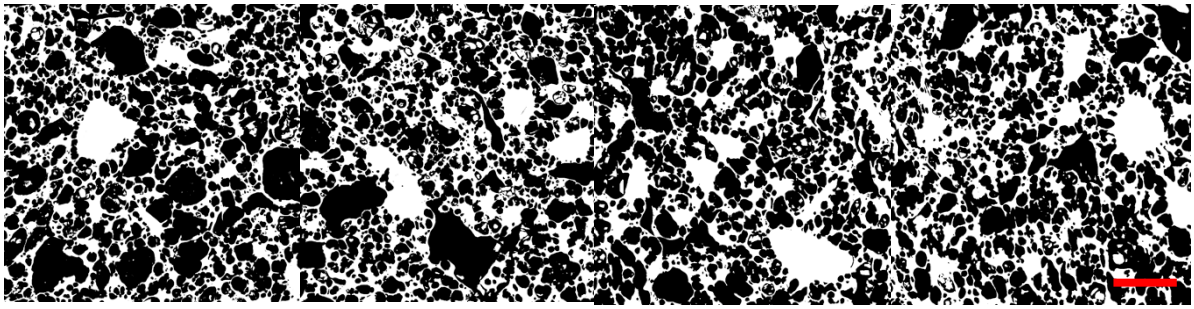

250x Images

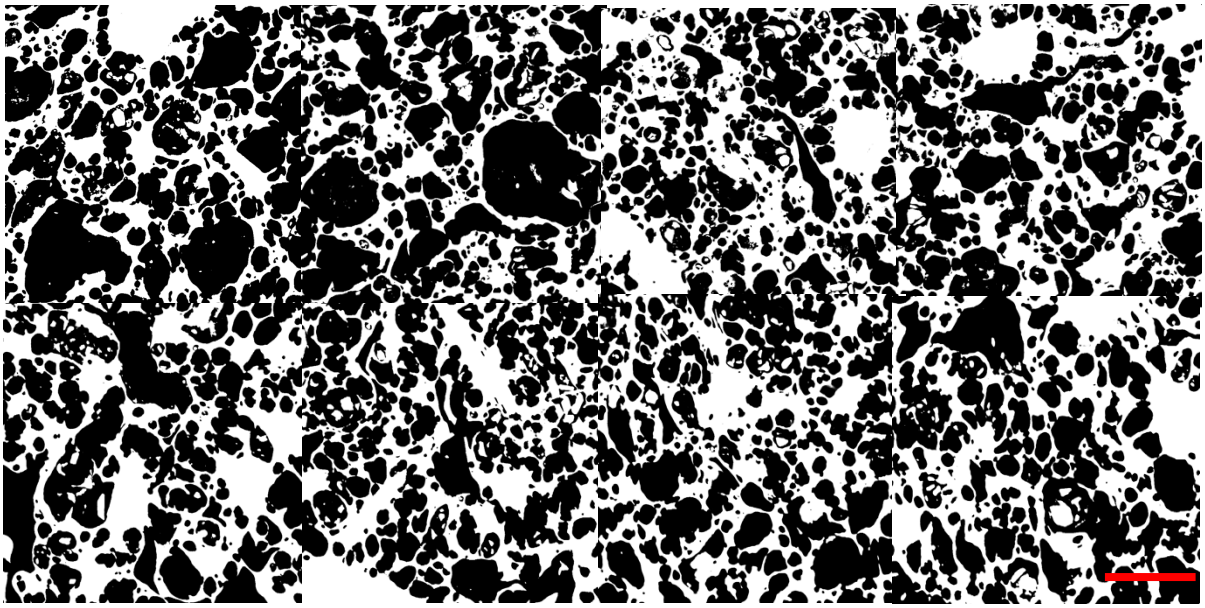

450x Images

Supplementary Figure 3: Edited BSE images for the top layer of the eruption.

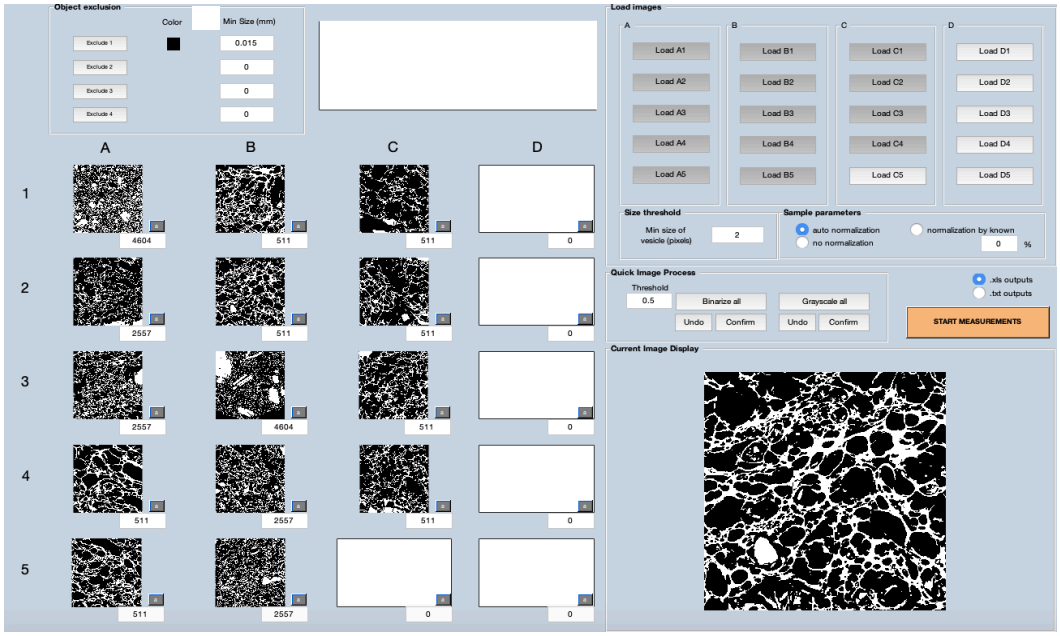

Example input of all bottom layer images into FOAMS.

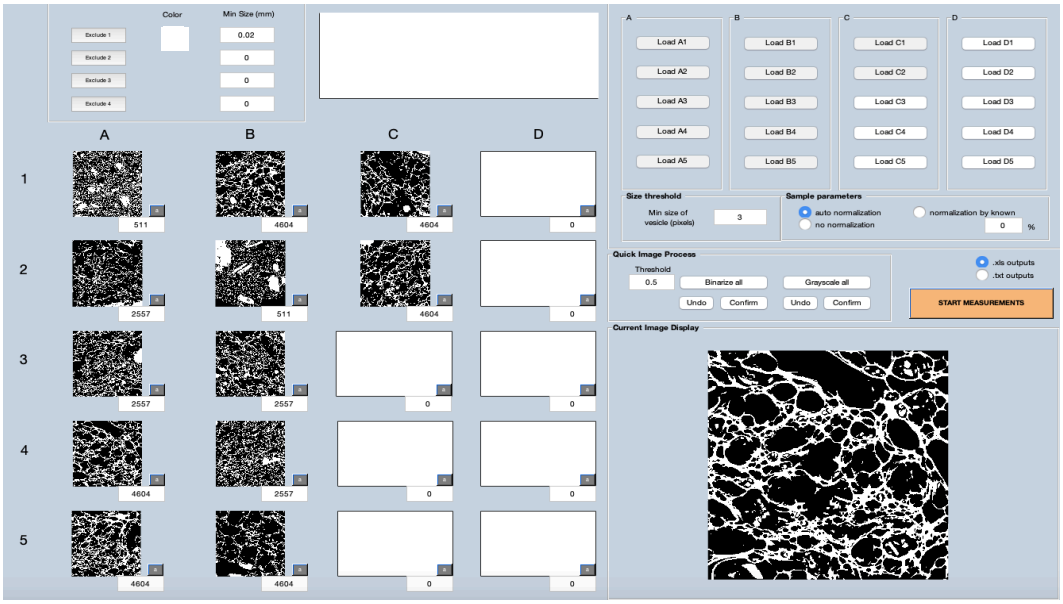

Example input of bottom images into FOAMS. Two 450x images are not included.

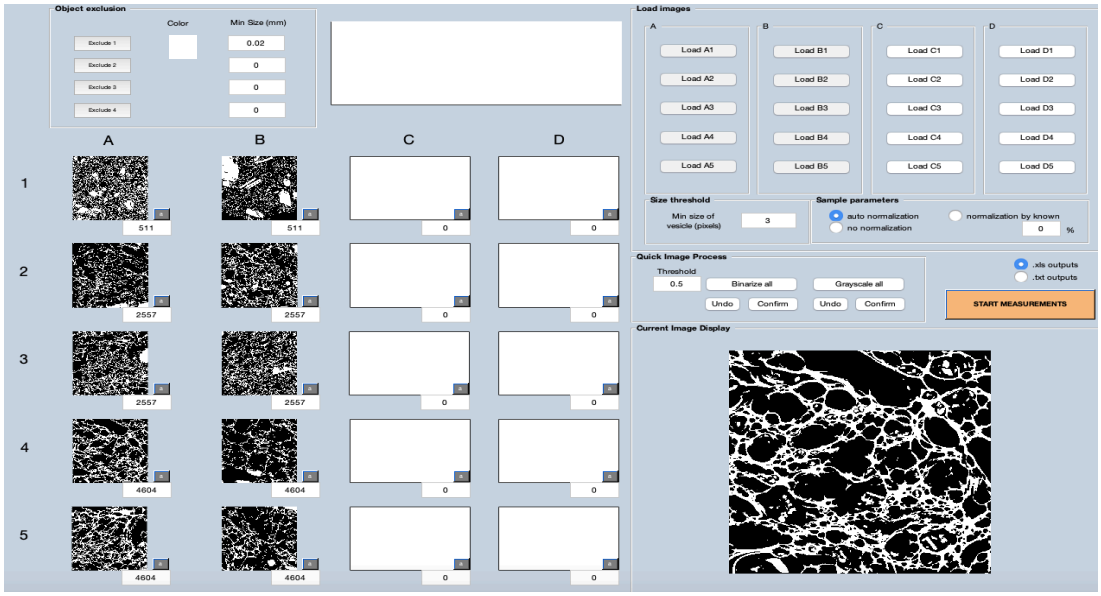

Example input of bottom images into FOAMS. Four 450x images are not included.

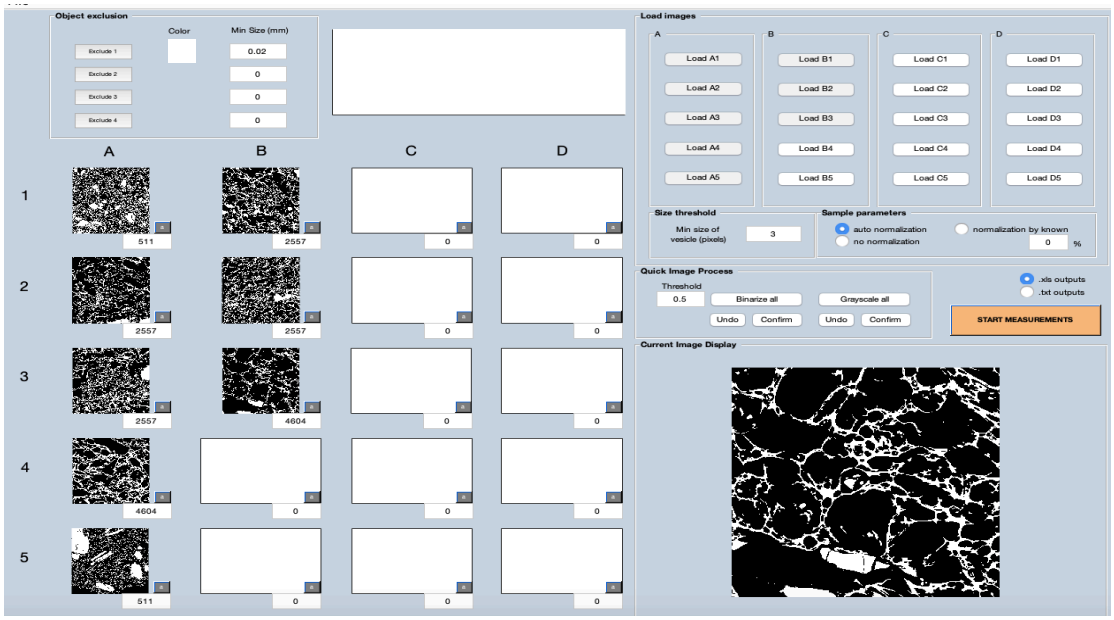

Example input of bottom images into FOAMS. Six 450x images are not included.

Supplementary Figure 4: Example of bottom layer input experiment to remove sequentially the images at the 450x magnification to assess uncertainty.